

# Topological Defects in Hyperbranched Glycopolymers Enhance Binding to Lectins

Miriam Salvadó,<sup>[a]</sup> José J. Reina,<sup>[b]</sup> Javier Rojo,<sup>[b]</sup> Sergio Castellón,<sup>[a]</sup> and Omar Boutureira<sup>\*[a]</sup>

**Abstract:** Central scaffold topology and carbohydrate density are important features in determining both the binding mechanism and potency of synthetic multivalent, polydisperse vs. monodisperse carbohydrate systems to a model plant toxin (RCA<sub>120</sub>). We found lower densities of protein receptors favour the use of heterogeneous, polydisperse glycoconjugate presentations as determined by surface plasmon resonance (SPR) and dynamic light scattering (DLS).

congested high-generation glycoconjugates<sup>[4]</sup> driving the attention to alternative, heterogeneous multivalent structures both at the

## Introduction

The complexity of cellular glycocalyx has been shaped over millions of year of evolution by the action of cell's (glyco)machinery, an intricate pool of carbohydrate-processing enzymes that together with a different set of post-translational modifications define the composition of the cellular membrane, and its components. Biological systems, and particularly glycoproteins, are heterogeneous in nature, yet the functions of redundant glycoforms, which represent structurally similar glycoproteins that differ in sugar structure, density, and/or glycosylation site, and decorate the outer surface of cells remains unknown. *Heterogeneous* glycoforms typically participate in a variety of surface recognition events. In one example, galectins are able to recruit and cross-link a heterogeneous collection of complex glycoconjugates that trigger important signalling events.<sup>[1–11]</sup> In another example, the presence of partially deglycosylated mucin proteins correlates with disease states *via* reduction of the high-density shell surface that reveals truncated, short epitopes (e.g. Tn and STn antigens). The presence of such composition and spatial organization defects enables preferential binding modes with particular lectins and reveals higher-order/supramolecular recognition patterns.<sup>[2]</sup> Thus, glycoproteins resulting from aberrant glycosylation patterns and/or with glycosylation defects render otherwise hidden structures surface exposed and sufficiently accessible to bind entities such as antibodies, lectins or pathogens with particularly high avidities (Figure 1a,b). Chemical glycobiochemists have traditionally focused their efforts on the development of homogeneous multivalent structures to precisely determine carbohydrate-protein binding events.<sup>[3]</sup> However, recent findings demonstrate that steric clash usually diminishes potency of homogeneous, yet sterically

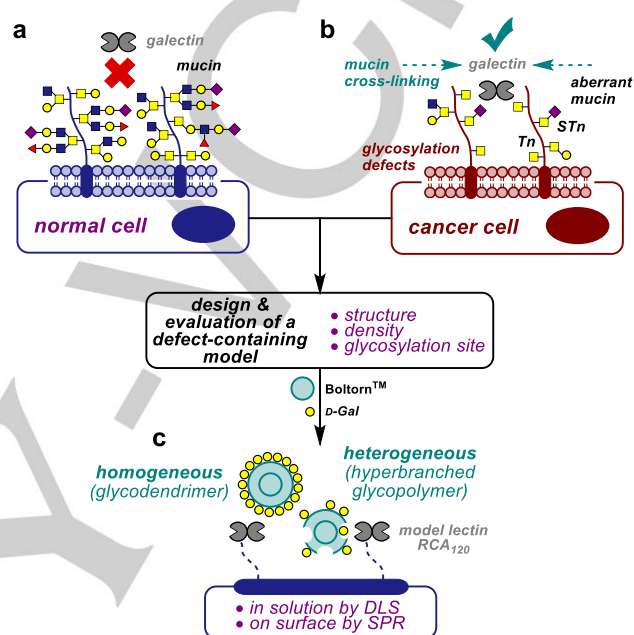


**Figure 1.** Schematic representation of the binding modes of (a) normal and (b) cancer cells to galectins due to the reduction/alteration of the surface glycan shell. (c) Proposed simplified model to evaluate binding mechanism and potency of both states.

glycan level<sup>[5]</sup> and the central core architecture.<sup>[6]</sup> Examples by Cloninger and co-workers highlight the presence of topological defects that enhance binding towards their targeted receptors.<sup>[7]</sup> In an attempt to mimic Nature and gain insight into the heterogeneous essence of multivalent sugar-protein interactions we sought to systematically evaluate the binding mechanism between a series of multivalent homogeneous (monodisperse) vs. heterogeneously (polydisperse) presented glycoligands and a model plant toxin (RCA<sub>120</sub>). We performed a thorough analysis *via* surface plasmon resonance (SPR) and dynamic light scattering (DLS) of the behaviour of readily accessible-processable hyperbranched glycopolymers<sup>[8]</sup> as a suitable family of simplified defect-containing multivalent glycomaterials with enhanced potency (Figure 1c). These two techniques are representative of surface vs. solution evaluation methods, two of the main important sugar-protein binding events occurring in Nature.

## Results and Discussion

A series of multivalent systems were synthesized using two different polyester polyol central cores (hyperbranched Boltorn™

[a] Dr. M. Salvadó, Prof. S. Castellón, Dr. O. Boutureira  
Departament de Química Analítica i Química Orgànica  
Universitat Rovira i Virgili  
C/ Marcel·lí Domingo 1, 43007 Tarragona (Spain)  
E-mail: omar.boutureira@urv.cat

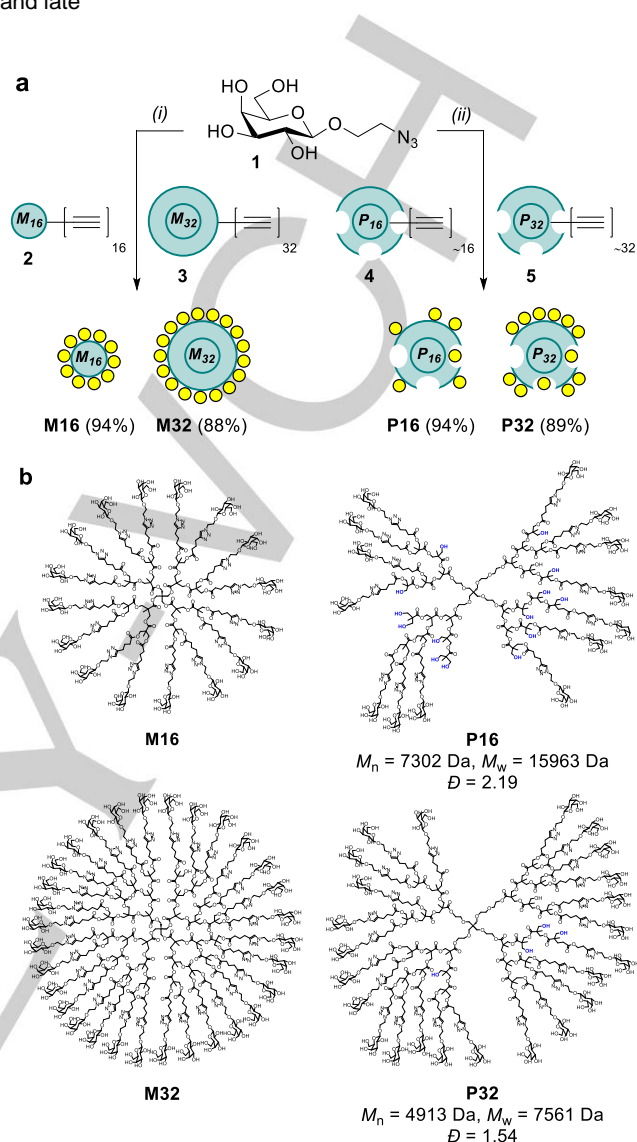
[b] Dr. J. J. Reina, Dr. J. Rojo  
Glycosystems Laboratory, Instituto de Investigaciones Químicas  
(IIQ), CSIC – Universidad de Sevilla, Av. Américo Vespucio 49,  
41092 Sevilla (Spain)

Supporting information and the ORCID identification number(s) for the author(s) of this article can be found under:

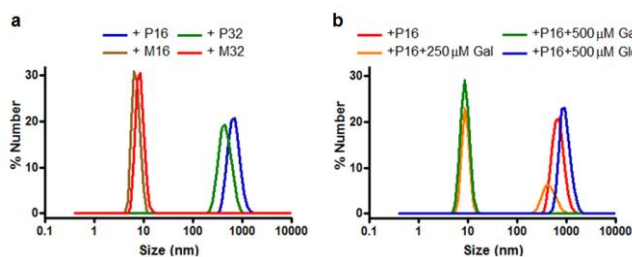
## FULL PAPER

H30 and pentaerythritol dendrimer) that allowed for the presentation of two different D-galactose loadings (16 and 32 D-Gal) in a monodisperse and a polydisperse manner (Scheme 1). Thus, glycosyl azide **1** was reacted with monodisperse **2**, **3** and polydisperse **4**, **5** alkyne cores to obtain **M16**, **M32** and **P16** (dispersity ( $\bar{D}$ ) = 2.19), **P32** ( $\bar{D}$  = 1.54), respectively (supporting information, Figures S13 and S14). We first investigated the aggregation properties and specificity of RCA<sub>120</sub> towards polydisperse and monodisperse ligands in solution by DLS (Figure 2). *Ricinus communis agglutinin* (RCA<sub>120</sub>) is a heterodimeric D-Gal-specific lectin with four subunits and a BAAB composition. Whereas in A-chain resides the cytotoxic activity, the B-chain contains two D-Gal-binding sites separated by ca. 100 Å and composed by two globular domains.<sup>[9]</sup> Both lectin and ligands (**P16**, **P32**, **M16**, and **M32**) were checked prior to analysis to determine their size and confirm the absence of aggregates (supporting information, Figure S4). A solution of RCA<sub>120</sub> (166 nM,  $D_h$  = 6.5 nm) in HBS-EP buffer was treated with increasing ligand concentrations (100–400 nM). At high concentrations, the only aggregates formed were those with polydisperse ligands, **P16** ( $D_h$  = 712 nm) and **P32** ( $D_h$  = 460 nm) while no aggregates were observed for monodisperse ligands, **M16** and **M32** supporting the fact under same concentration range and generation, polydisperse ligands proved more effective to cross-link RCA<sub>120</sub> (Figure 2a). For **P32**, the largest aggregates were observed at 200 nM (1:1.2 lectin/ligand ratio), confirming that the ligand was acting as the nucleating agent<sup>[10]</sup> while no aggregates were found for monodisperse ligands presenting a similar carbohydrate loading. A series of control experiments were also performed to confirm the binding specificity of RCA<sub>120</sub> towards D-Gal residues (Figure 2b). A solution of **P16** with RCA<sub>120</sub> in HBS-EP buffer (1:2.4 lectin/ligand ratio) was chosen for the study. The solution was titrated with D-galactose (from 250 μM to 1 mM) and the particle size was determined. For concentrations of D-galactose up to 500 μM, reversion of aggregate formation was observed. While titration of the same solution with the same amount of D-glucose as well as the equivalent volume of buffer (HBS-EP) did not influence aggregate formation, indicating that our ligands were able to bind selectively to RCA<sub>120</sub> due to the presence of non-reducing D-Gal residues (supporting information, Figure S6). With these preliminary results in hand, we sought to study how the monodisperse and polydisperse D-Gal presentation significantly influences the binding kinetics and mechanism. To obtain kinetic data of multivalent interactions, SPR direct binding experiments were performed (Table 1). RCA<sub>120</sub> was covalently attached to a polycarboxyl CM5 sensor chip to generate three different lectin surfaces at various levels of functionalization (RCA<sub>120</sub>-HD, -MD, and -LD where HD, MD, and LD = high, medium, and low densities, respectively). Binding data were collected at 5 μL/min flow rate using different analyte concentrations. Prior to analysis, binding tests using RCA<sub>120</sub>-HD at different flow rates were performed to discard mass transport effects that could influence the shape of sensograms.<sup>[11]</sup> As expected, complex binding profiles were reflected in sensograms with RCA<sub>120</sub>-MD (chosen for further studies due to easier surface regeneration) according to the multivalent nature of the analytes tested. Attempts to fit the results obtained to conventional binding models failed, yet following the procedure described by Fernandez-Megia *et al.*,<sup>[12]</sup>

a separate kinetic analysis of the sensograms at early association and late



**Scheme 1.** (a) Preparation of multivalent (glyco)polymers/dendrimers; (i) CuSO<sub>4</sub>·5H<sub>2</sub>O, NaAsc, TBTA, 1:1 THF/H<sub>2</sub>O, microwave (μwave) irradiated in a sealed tube at 60 °C for 2 h using a CEM-Discover™ single-mode synthesizer (temperature control, fixed hold time off, normal absorption mode, 300 W); (ii) CuSO<sub>4</sub>·5H<sub>2</sub>O, NaAsc, 1:1 tBuOH/H<sub>2</sub>O, rt, 72 h for **P16** and CuSO<sub>4</sub>·5H<sub>2</sub>O, NaAsc, TBTA, 1:1 THF/H<sub>2</sub>O, μwave, 60 °C, 2 h for **P32**. (b) Structures of monodisperse dendrimers (**M16**, **M32**) and idealized polydisperse hyperbranched polymers (**P16**, **P32**). NaAsc = sodium ascorbate. TBTA = tris[(1-benzyl-1*H*-1,2,3-triazol-4-yl)methyl]amine.



## FULL PAPER

**Figure 2.** Particle size measurements by DLS using (a) RCA<sub>120</sub>/ligands (1:2.4 ratio) in HBS-EP buffer and (b) titrations of RCA<sub>120</sub>/P16 with D-Gal and D-Glc.

**Table 1.** Kinetic data of the binding of multivalent M/P-Gal<sub>n</sub> ligands to RCA<sub>120</sub> surfaces with low density (LD) and medium density (MD).  $k_{on}$  ( $\times 10^4 \text{ M}^{-1} \text{ s}^{-1}$ ),  $k_{off}$  ( $\times 10^4 \text{ s}^{-1}$ ) and  $K_D$  (nM).

Ligand	RCA <sub>120</sub> -LD (1300 RU) <sup>[a]</sup>			RCA <sub>120</sub> -MD (6400 RU) <sup>[b]</sup>			
	$k_{on}$	$k_{off}$	$K_D$	$k_{on1}$	$k_{on2}$	$k_{off}$	$K_D$
<b>P16</b>	1.44	17.9	125	10.6	1.93	6.35	11.7
<b>M16</b>	ND	ND	ND	217	24.9	56.2	3.23
<b>P32</b>	13.8	45	32.6	57.5	8.0	8.73	2.71
<b>M32</b>	ND	ND	ND	66.7	9.21	18.6	5.93

<sup>[a]</sup> Fitted to a 1:1 Langmuir binding model. <sup>[b]</sup> Separate kinetic analysis of early association and late dissociation phases. ND=not detected (the analyte does not remain attached to the chip surface after injection and therefore the increase in RUs during association is due to a change in the refractive index caused by the change in solution concentration).

dissociation phases was performed (Figure 3 and supporting information, Figures S1 and S2). During the dissociation, a two-phase process was observed. Initially a fast dissociation was shown followed by an extremely slow dissociation phase suggesting the presence of both weak and strong binding events. This fast dissociation is more pronounced in monodisperse than in polydisperse analytes. More analyte remains attached to the surface of the lectin when polydisperse structures are tested. In both cases, attempts to fit the dissociation phase to conventional binding models failed. While the major degree of heterogeneity was found at early dissociation times ( $t = 180\text{--}250 \text{ s}$ ), late dissociation times ( $t \geq 250 \text{ s}$ ) showed good fitting to a 1:1 Langmuir binding model. For polydisperse analytes,  $k_{off}$  values were found to be lower than for monodisperse. Significantly different values in  $k_{off}$  resulted when comparing multivalent structures presenting the same number of D-Gal units. **M16** and **M32** showed 8.9- and 2.1-fold higher dissociation rates than **P16** and **P32**, respectively. When comparing dispersity, in the case of polydisperse analytes (**P16** and **P32**) a 1.4-fold slower dissociation was observed when the number of D-Gal was increased (Table 1). In contrast, **M16** showed a 3.0-fold slower dissociation than the corresponding 3<sup>rd</sup> generation monodisperse **M32**. The same trend was observed for polydisperse **P16** when the early dissociation phase was evaluated as the percentage of SPR signal decay ( $t = 180\text{--}250 \text{ s}$ ). For **P16** the percentage observed was 1.9- and 1.1-fold lower than for **P32** and **M16** (supporting information, Table S1). The slow dissociation of polydisperse Boltorn<sup>TM</sup> structures (**P16** and **P32**) and their low percentage of signal decay from RCA<sub>120</sub>-MD surface represented an enhanced binding activity compared to monodisperse structures (**M16** and **M32**). The significant low value of off rates could be explained because a nearby analyte could quickly replace a bound analyte in close proximity (statistical rebinding), which is favoured when D-Gal is presented to the receptor in a polydisperse manner due to the higher accessibility of the sugar epitopes compared to those found in more crowded, sterically congested monodisperse systems. Additional stabilization due to the presence of secondary interactions with unmodified surface groups and/or inner core may also affect off rates. After an

exhaustive evaluation of the dissociation phase of the sensogram, a kinetic evaluation of the association was also performed. The linear increase observed during the association phase, also indicates a strong binding. The early association phase ( $t \leq 50 \text{ s}$ ) was fitted to a 1:1 Langmuir binding model and  $k_{obs}$  vs. concentration was plotted. Deviations from the linear behaviour were found for all analytes

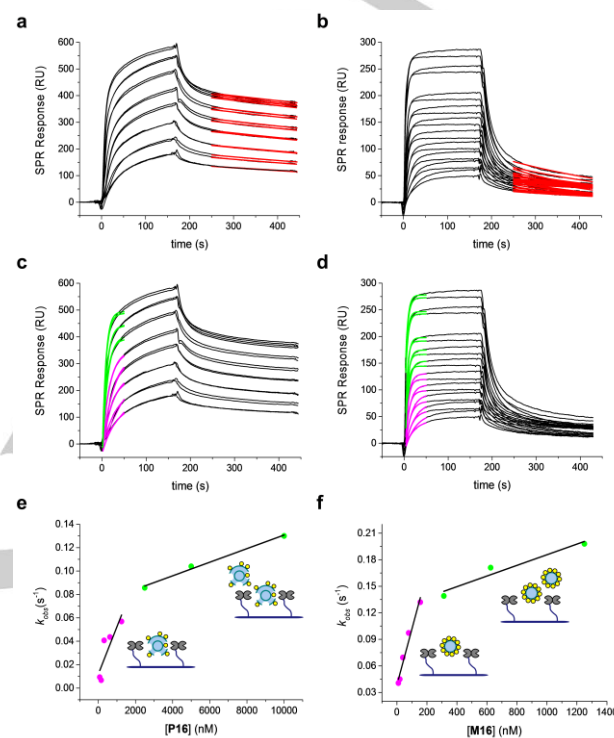


**Figure 3.** Representative SPR separate kinetic analysis of the interaction of **P16** and **M16** with RCA<sub>120</sub>-MD. (a, b) Late dissociation phase kinetic analysis: sensograms and global fitting (red) to pseudo-first-order kinetics. (c, d) Early association phase kinetic analysis: sensograms and global fitting of the early association phase (magenta and green) to the integrated rate equation for pseudo-first-order kinetics. (e, f) Plots of  $k_{obs}$  vs. [ligand].

evaluated and two different slopes were observed (Figure 3 and supporting information, Figures S1 and S2). Low concentrations present a fast association (largest slope, high order complexes) while high concentrations present a slow association resulting in complex kinetic interactions due to the multivalent nature of the analytes (Table 1). The 2-fold increase of D-Gal residues in polydisperse analytes (from **P16** to **P32**) resulted in a 5-fold increase in  $k_{on1}$ . This trend was not observed in monodisperse analytes, when the glycodendrimer surface is coated with 32 D-Gal units  $k_{on1}$  value for **M32** ( $66.7 \times 10^4 \text{ M}^{-1} \text{ s}^{-1}$ ) decreased in 3.2-fold compared to **M16** ( $217 \times 10^4 \text{ M}^{-1} \text{ s}^{-1}$ ), which at low concentrations yielded a  $k_{on1}$  value 20.4-fold higher than **P16** ( $10.6 \times 10^4 \text{ M}^{-1} \text{ s}^{-1}$ ) and a  $k_{on2}$  ( $24.9 \times 10^4 \text{ M}^{-1} \text{ s}^{-1}$ ) 12.9-fold higher at high concentrations. For **M32**,  $k_{on1}$  and  $k_{on2}$  were only 1.2-fold higher compared to **P32**. The shape of sensograms was indicative of the high increase of binding for monodisperse compared to polydisperse analytes (at early association a more pronounced increase is observed in **M16** and **M32** sensograms compared to

**P16** and **P32**). In hyperbranched polymers (**P**), when the number of carbohydrates presented in the surface increases their effective multivalency is also amplified. This effect could favor rebinding processes and the fact that one analyte could simultaneously bind to two proteins might explain why the affinity constant increase when the number of carbohydrates presented is higher. However in the case of homogeneous glycodendrimers it is known that structures with higher generations (high valency) not always give better affinities.<sup>[13]</sup> The drop in affinity has been usually attributed to steric hindrance between carbohydrate units. In previous studies the binding constant of D-galactose towards RCA<sub>120</sub> has been determined by isothermal titration calorimetry (ITC) with a  $K_D$  of  $4.5 \times 10^{-4}$  M.<sup>[14]</sup> **P16**, **M16**, **P32**, and **M32** yielded a  $K_D$  in the nM range, four orders of magnitude lower than its monomeric counterpart. These results suggest that our multivalent ligands are able to simultaneously bind two RCA<sub>120</sub> lectins in the MD-surface.<sup>[15]</sup> The detailed kinetic evaluation of RCA<sub>120</sub>-MD gave important information about the real-time binding of this type of analytes, showing a heterogeneous binding with distinguishable weak and strong affinities caused by clustering and rebinding phenomena. SPR direct binding analysis was also performed in RCA<sub>120</sub>-LD for our four analytes, yet conversely to MD-surface no binding was detected for monodisperse ligands (Table 1). Exhaustive analysis of the polydisperse analytes was also performed at different concentrations. The same sensogram profile was observed as that for RCA<sub>120</sub>-MD. According to the dissociation and association phases, the same trend is observed as in RCA<sub>120</sub>-MD, a fast dissociation followed by a slow dissociation and a linear increase in association. However, the decrease in lectin density showed a less complex binding profile and the sensograms could be fitted well to a 1:1 Langmuir binding model. Thus, the RCA<sub>120</sub>-LD surface showed a single slope that equals to  $K_{on}$  when plotting  $K_{obs}$  vs. concentration for **P16** and **P32** indicating no binding heterogeneity (supporting information, Figure S3). The binding efficiency between generations is maintained but the decrease in lectin density impedes the analyte to simultaneously bind two RCA<sub>120</sub> lectins. The high affinity binding modes could only be explained by rebinding and clustering with the lectin secondary

binding sites. Thus, the study of the binding affinities with different lectin density gave an idea of the importance of sugar presentation vs. mode of action. Accordingly, this real-time-dependent analysis suggests that the different binding mechanisms described depend on the local concentration of analyte and its proximity to the immobilized lectin and not only to the analyte multivalency and the lectin surface density.

## Conclusions

In summary, we found the nature of the core and the display of ligands enormously affects the binding mechanism and potency.<sup>[4]</sup> Modifications of the central core of multivalent systems give relevant binding differences in both DLS and SPR experiments. Thus, lower densities of receptors (RCA<sub>120</sub>) as those found in physiological environments favour the use of heterogeneous (polydisperse) glycoconjugate presentations – mimicking inherent defects found in glycoproteins and/or different glycoforms – that enhance their potency in a match scenario of interactions suggesting this mutual reinforcement might be one of the pivotal reasons for the co-evolution of glycans to such complex, heterogeneous structures. We anticipate the data presented herein will be relevant to develop cheap, ready available multivalent carbohydrate therapeutics designed and utilized as anti-infective agents against common human diseases.

## Acknowledgements

We thank the European Commission (Marie Curie CIG, O.B.), MINECO (CTQ2014-58664-R, CTQ2014-52328-P, and RYC-2015-17705), the European Regional Development Fund, Generalitat de Catalunya (M.S.), and CSIC (JAEdoc contract, J.J.R.) for financial support. O.B. is a Ramón y Cajal Fellow.

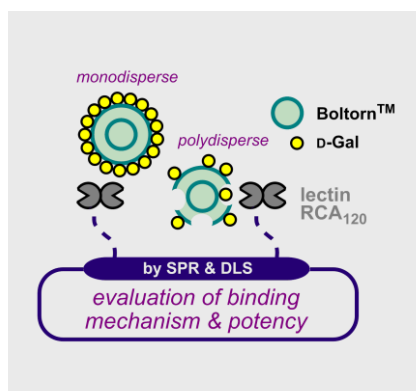
**Keywords:** carbohydrates • glycodendrimers • hyperbranched glycopolymers • molecular recognition • multivalency

- [1] B. Belardi, G. P. O'Donoghue, A. W. Smith, J. T. Groves, C. R. Bertozzi, *J. Am. Chem. Soc.* **2012**, *134*, 9549–9552.
- [2] K. Godula, C. R. Bertozzi, *J. Am. Chem. Soc.* **2012**, *134*, 15732–15742.
- [3] a) S. Cecioni, A. Imberty, S. Vidal, *Chem. Rev.* **2015**, *115*, 525–561; b) Y. M. Chabre, R. Roy, *Chem. Soc. Rev.* **2013**, *42*, 4657–4708.
- [4] a) S. Bhatia, L. Cuellar Camacho, R. Haag, *J. Am. Chem. Soc.* **2016**, *138*, 8654–8666; b) M. Kanai, K. H. Mortell, L. L. Kiessling, *J. Am. Chem. Soc.* **1997**, *119*, 9931–9932; c) P. R. Ashton, E. F. Hounsell, N. Jayaraman, T. M. Nilsen, N. Spencer, J. F. Stoddart, M. Young, *J. Org. Chem.* **1998**, *63*, 3429–3437; d) D. Pagé, R. Roy, *Bioconjugate Chem.* **1997**, *8*, 714–723.
- [5] a) J. L. Jiménez Blanco, C. Ortiz Mellet, J. M. García Fernández, *Chem. Soc. Rev.* **2013**, *42*, 4518–4531; b) D. Ponader, P. Maffre, J. Aretz, D. Pussak, N. M. Ninnemann, S. Schmidt, P. H. Seeberger, C. Rademacher, G. U. Nienhaus, L. Hartmann, *J. Am. Chem. Soc.* **2014**, *136*, 2008–2016; c) L. Xue, X. Xiong, K. Chen, Y. Luan, G. Chen, H. Chen, *Polym. Chem.* **2016**, *7*, 4263–271.
- [6] a) Y. Miura, Y. Hoshino, H. Seto, *Chem. Rev.* **2016**, *116*, 1673–1692; b) E. Schaeffer, L. Dehuyser, D. Sigwalt, V. Flacher, S. Bernacchi, O.

- Chaloin, J.-S. Remy, C. G. Mueller, R. Baati, A. Wagner, *Bioconjugate Chem.* **2013**, *24*, 1813–1823.
- [7] E. K. Woller, E. D. Walter, J. R. Morgan, D. J. Singel, M. J. Cloninger, *J. Am. Chem. Soc.* **2003**, *125*, 8820–8826.
- [8] C. C. Lee, J. A. MacKay, J. M. J. Fréchet, F. C. Szoka, *Nat. Biotechnol.* **2005**, *23*, 1517–1526.
- [9] a) C. Scheibe, S. Wedepohl, S. B. Riese, J. Dervede, O. Seitz, *ChemBioChem* **2013**, *14*, 236–250; b) V. Wittmann, R. J. Pieters, *Chem. Soc. Rev.* **2013**, *42*, 4492–4503.
- [10] C. K. Goodman, M. L. Wolfenden, P. Nangia-Makker, A. K. Michel, A. Raz, M. J. Cloninger, *Beilstein J. Org. Chem.* **2014**, *10*, 1570–1577.
- [11] D. G. Myszka, *Curr. Opin. Biotech.* **1997**, *8*, 50–57.
- [12] E. M. Munoz, J. Correa, R. Riguera, E. Fernandez-Megia, *J. Am. Chem. Soc.* **2013**, *16*, 5966–5969.
- [13] F. Lasala, E. Arce, J. R. Otero, J. Rojo, R. Delgado, *Antimicrob. Agents Chemother.* **2013**, *47*, 3970–3972.
- [14] T. K. Dam, C. F. Brewer, *Chem. Rev.* **2002**, *102*, 387–430.
- [15] a) A. Mulder, T. Auletta, A. Sartori, S. Del Ciotto, A. Casnati, R. Ungaro, J. Huskens, D. N. Reinhoudt, *J. Am. Chem. Soc.* **2004**, *126*, 6627–6636; b) M. Mammen, S.-K. Choi, G. M. Whitesides, *Angew. Chem. Int. Ed.* **1998**, *37*, 2754–2794; *Angew. Chem.* **1998**, *110*, 2908–2953.

## FULL PAPER

Core topology and sugar density in synthetic multivalent, polydisperse vs. monodisperse carbohydrate structures affect binding mechanism and potency to a model plant toxin



M. Salvadó, J. J. Reina, J. Rojo, S. Castellón, O. Boutureira\*

Page No. – Page No.

Topological Defects in Hyperbranched Glycopolymers Enhance Binding to Lectins